JOURNAL OF MATERIALS SCIENCE 29 (1994) 4618–4624

Creep features of Al_2O_3–Al alloy composites

X. C. LIU, C. BATHIAS
Department of Mechanical Engineering, CNAM, 2 Rue Conté, 75003 Paris, France

Creep features of two cast aluminium alloy composites reinforced by Al_2O_3 short fibres randomly oriented in the matrices have been studied at 300 °C and several stress levels. The presence of short-term negative creep in primary creep is an important feature for the composites, which resulted from randomly oriented fibres strongly resisting dislocation creep in the matrix. However, the negative creep magnitude depended on both the applied stress and the nature of the material. There was a critical stress for the presence of the short-term negative creep. When the applied stress had exceeded the critical value, the negative creep disappeared. Fibres traversing grain boundaries can reinforce and resist grain boundary sliding at elevated temperature. The effect of stress on creep rate for the composites is not so strong as that for unidirectional metallic matrix composites. During the creep, some intermetallic phases in the Al_2O_3/Al–5Si–3Cu-1Mg composite were precipitated and most of them were segregated at grain boundaries, leading to a small increase of the creep rate.

1. Introduction

Metallic matrix composites (MMCs) are a class of potential materials that can be used at elevated temperature. The incorporation of a higher melting-point reinforcement can substantially increase the temperature capability relative to that of the matrix alone; for example, commercial aluminium alloys are restricted to structural applications at temperatures below about 200 °C, but the incorporation of 10–20% by volume of SiC fibre in an aluminium matrix allows a similar short-term strength to be retained to maximum temperatures of about 400 °C or even more elevated temperatures [1]. Most of the structural materials are intended for use for a long time, so shape changing arising from creep are generally undesirable and can be the limiting factor in the life of a part. For example, blades on the spinning rotors in turbine engines slowly grow in length during operation and must be replaced before they touch the housing; thus it is important to estimate the long-term stability of such materials under stress at elevated temperatures.

Some models for the creep of unidirectional fibre MMCs, with short or long fibres, and loaded in or off the fibre directions, have been described without considering the effect of the fibre–matrix (F–M) interface [2–7]. Considered the effects of F–M interfaces on creep deformation, Goto and McLean [8, 9] described a creep model for unidirectional fibre-reinforced MMC. They concluded that weak interfaces had a very large effect on the creep behaviour of aligned short-fibre composites, but no significant effect on creep performance of continuous-fibre composites. Nieh [10] and Lilholt and Taya [11] studied the creep behaviour of SiCw/2024 and SiCw/6061 composites, respectively, in which the whiskers were aligned. It was concluded that the minimum creep rate for the composites was strongly dependent on the applied stress.

Evidently, the orientation and dimensions of fibres in a composite are important factors for the creep characteristics. However, few published papers on the creep of random orientation short-fibre MMCs can be found. The present paper deals with the creep of two random orientation alumina short-fibre cast aluminium alloy composites. Most of our attention is paid to short-term negative creep and the roles of randomly oriented fibres in the course of creep.

2. Experimental procedure

Two random short-fibre composite materials with a fibre volume of 20%, Al_2O_3/Al–7Si–0.6Mg and Al_2O_3/Al–5Si–3Cu–1Mg (in wt%), were used. The structure and properties of the fibre and the chemical compositions of the matrices are presented in Table I and II respectively. The composites were manufactured by the method of squeeze casting. After casting, they were subsequently subjected to the following heat treatment:

(i) For Al_2O_3/Al–5Si–3Cu–1Mg: 6 h at 510 °C + water quench (70 °C) + 6 h at 160 °C;

(ii) For Al_2O_3/Al–7Si–0.6Mg; 6 h at 540 °C + water quench (25 °C) + 6 h at 160 °C.

TABLE I Characteristics of SAFFIL Al_2O_3 fibres

Composition	Al_2O_3: 97%, SiO_2: 3%
Crystal structure	δ-Al_2O_3 (polycrystalline)
Density	3.3
Thermal expansion coefficient	$8 \times 10^{-6}\,°C^{-1}$
Mean length	150 μm
Mean diameter	3 μm
Service temperature	< 1600 °C
Strength	2000 MPa
Strain to failure	0.67%
Elastic modulus	300 GPa

0022–2461

TABLE II Chemical composition of matrices

	Fe	Si	Cu	Mg	Mn	Ni	Pb	Sn	Ti	Zn	Al
Al–5Si–3Cu–1Mg	0.21	5.56	3.39	1.28	0.31	0.008	0.01	0.02	0.08	0.03	Bal,
Al–7Si–0.6Mg	0.25	7.06	0.01	0.57	0.02	0.007	0.007	0.03	0.16	0.03	Bal.

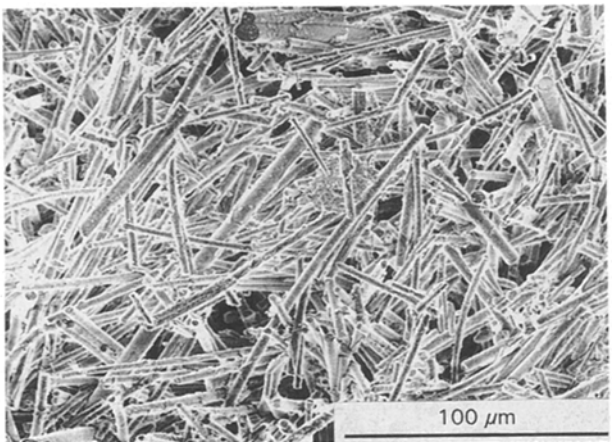

Figure 1 Fibre orientation in the composites (deeply etched sample). × 500.

The typical microstructure and fibre orientation in the composites are shown in Fig. 1 and Fig. 2, respectively. From these, it is clear that fibre orientation in the matrix is almost random in three-dimensional space, and the dispersion of intermetallic phases or precipitates in the matrix is homogeneous.

For a conventional metallic material, if the creep test is effected at constant external tensile load rather than at constant stress, then the stress will constantly increase as the creep strain reduces the cross-sectional area of the specimen, and this can cause creep to accelerate. However, reduction of the cross-sectional area of the composite specimens used in our study during the creep tests was very small, so even through the creep tests were carried out at a constant external tensile load they can be considered to be done at a constant stress. The main difficulty in doing creep tests for this kind of material comes from their small deformation. In order to precisely detect creep deformation of the materials, an Instron 8501 machine was used which can determine the displacement with a precision of 1 μm. An induction heating instrument equipped with a precise temperature control system was used. The creep deformation–time curves were continually recorded in time through the whole creep test with a graphic recorder. The tests were conducted on dog-bone specimens at 300 °C and several stress levels. In order to determine the influence of applied load on creep deformation, some tests were carried out at several increased load levels on the same specimen and at the same temperature. Some specimens polished before the testing were examined by optical or electron microscopes before and after creep testing. The chemical composition changes at both grain boundary and F–M interfaces, and in the matrix, were analysed with an electron probe.

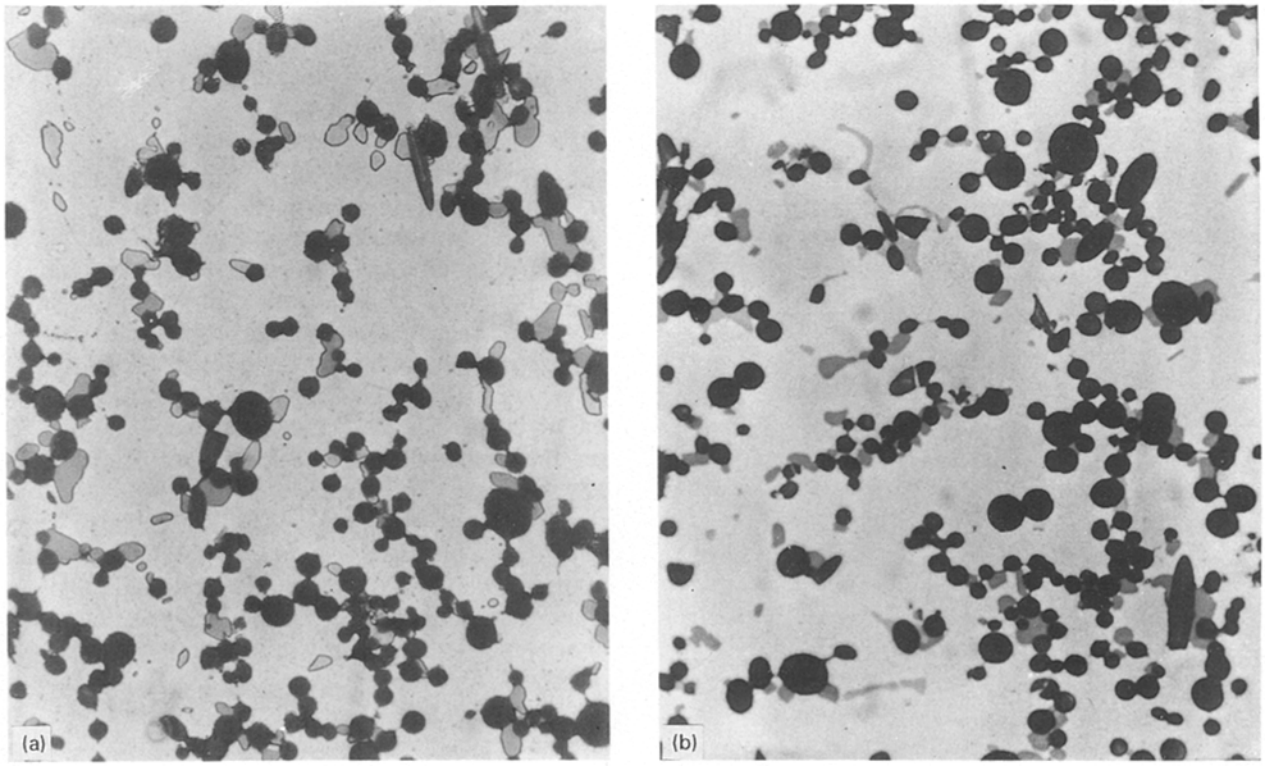

Figure 2 Microstructure of the composites (polished samples): (a) Al_2O_3/Al–5Si–3Cu–1Mg, (b)Al_2O_3/Al–7Si–0.6Mg. × 720.

3. Results and discussion

3.1. Creep curves

Typical deformation–time curves are presented in Fig. 3, from which can be seen a dominant primary creep, i.e. the deformation is mainly concentrated in the primary creep, and a stable secondary creep. Also it can be seen that after the deformation in primary creep had arrived at a maximum value, the specimen began to contract for a certain time; then the deformation started to increase again a phenomenon defined as short-term negative creep. Most of the curves show this kind of negative creep for the composites used in the study; however, as the applied load was increased the negative creep was reduced, and even disappeared as shown by Fig. 3b and c, respectively.

For a specimen with a band free of fibres, the band of which traversed most of the specimen cross-section as shown by the photo in Fig. 4, even when the load was not high there was neither negative creep nor secondary creep, and the deformation in ternary creep and total strain to failure were still very small.

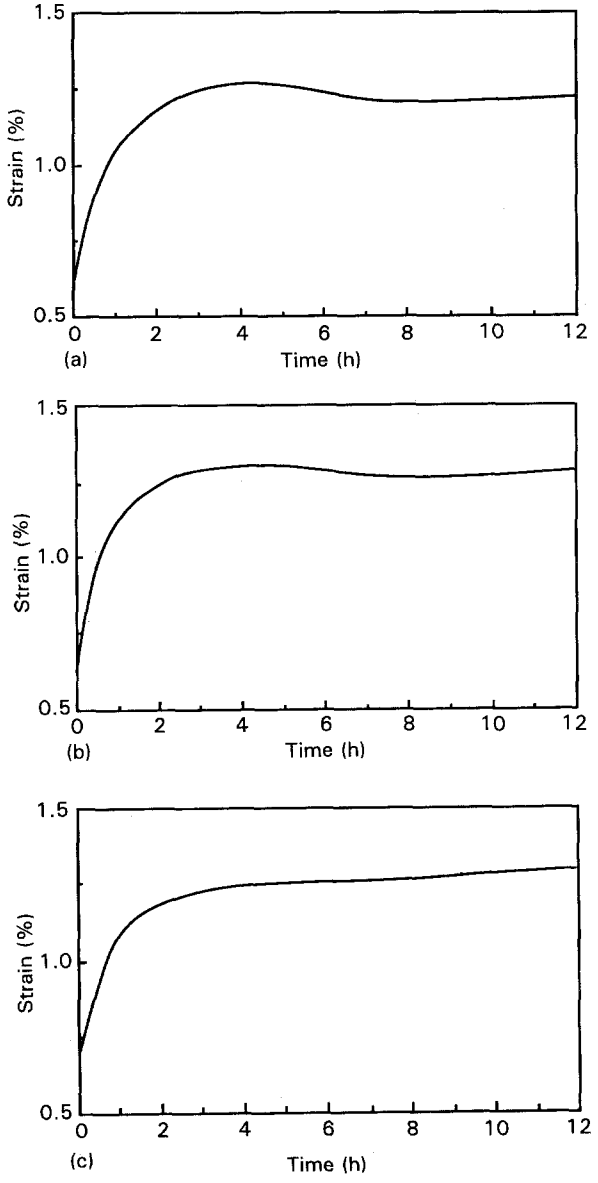

Figure 3 Typical creep curves at 300 °C: (a) noticeable negative creep (75 MPa, Al_2O_3/Al–5Si–3Cu–1Mg); (b) small negative creep (88 MPa, composite as (a)); (c) no negative creep at all (100 MPa, Al_2O_3/Al–7Si–0.6Mg).

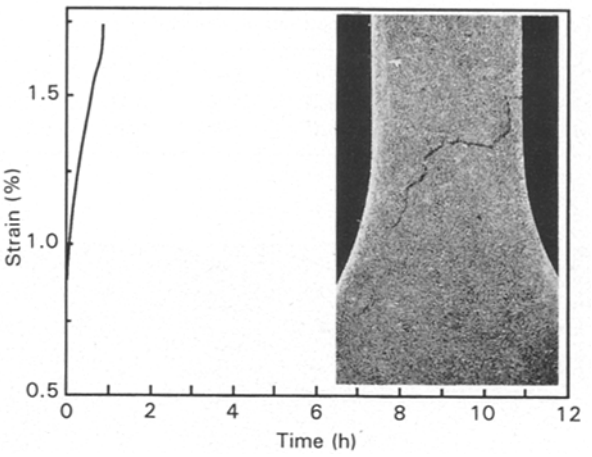

Figure 4 Creep Curve and photograph (×6) of specimen with a band free of fibres (black line in the photo) 300 °C, 95 MPa, Al_2O_3/Al–7Si–0.6Mg.

During creep, dislocations are created and forced to move through the material. This leads to work-hardening as the dislocation density increases and the dislocations encounter barriers to their motion. At low temperature, an ever-diminishing creep rate results; however, if the temperature is sufficiently high, dislocations rearrange and annihilate through recovery events. The combined action of hardening and recovery processes during primary creep can lead to negative creep in the case where the hardening action is dominant for a certain time. This short-term negative creep was also observed in tests on quenched and tempered 2.25Cr–1Mo steel at 482 and 538 °C for the same steel in the normalized and tempered condition [12]. When both hardening and recovery processes during primary creep are stable and in part compensate each other, a stable secondary creep develops.

Finally, it should be pointed out that there is no significant difference between the creep curves of the two composite materials. However, negative creep for the Al_2O_3/Al–7Si–0.6Mg composite was much smaller with respect to the Al_2O_3/Al–Si–3Cu–1Mg composite.

3.2. Steady-state creep rate

The most important creep parameter in terms of theoretical analysis is the steady-state creep rate, i.e. the minimum creep rate in the case without negative creep. The values of steady-state creep rate in secondary-creep for the composites at different stress level are presented in Table III. Apparently, the creep rate of the Al_2O_3/Al–5Si–3Cu–1Mg composite is a little larger than that of Al_2O_3/Al–7Si–0.6Mg. The steady-state creep rate 201.0 cast aluminium alloys at 290 °C and 90 MPa is 0.062% h^{-1} [13]. Roughly, the creep rate for the composites is smaller by almost one order of magnitude than that of the cast aluminium alloys alone. The difference between the creep rates of the two composites is evidently related to the nature of the matrices.

The dependence of steady-state creep rate ($\dot{\varepsilon}$) on stress at a given temperature is generally expressed as

$$\dot{\varepsilon} = k\sigma^n$$

TABLE III Mean creep properties of composites

	Al_2O_3/Al–7Si–0.6Mg			Al_2O_3/Al–5Si–3Cu–1Mg			
Applied stress (MPa)	100	88	75	55	95	88	75
Steady-state creep rate (%h^{-1})	0.015	0.009	0.006	0.002	0.018	0.011	0.007
Magnitude of negative creep in the gauge length (μm)	0.0	1.4	4.8	6.8	1.6	6.3	10.3

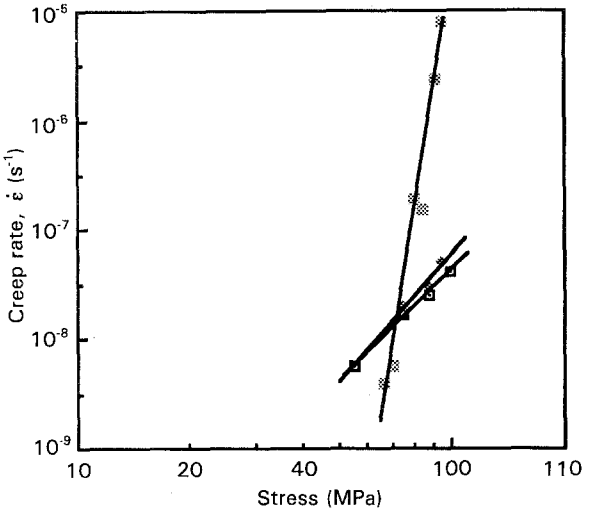

Figure 5 Creep rate of composites versus stress: (□) Al_2O_3/Al–7Si–0.6Mg (300 °C), (◆) Al_2O_3/Al–5Si–3Cu–1Mg (300 °C), (⋮⋮⋮) SiCw/6061 (291 °C) after Nieh [10].

where k is a constant, σ the applied stress and n the stress exponent for creep. For pure metals, n generally varies from 4 to 5, and for solid-solution alloys n has a value of approximately 3. For precipitation- or dispersion-strengthened alloys, or MMCs, the reported values of n can range as high as 30 to 40. Because of the theoretical developments, certain values of the stress exponent for creep have been correlated with deformation mechanisms. Such high values can be explained in terms of the interaction stresses between dislocations and the barriers to dislocation motion during creep. The steady-state creep rate as a function of stress is plotted in Fig. 5, where each point is the average of four test results, along with the results of Nieh [10] for comparison. The results of linear regression fits to power-law creep are given as follows:

$$\dot{\varepsilon} = 10^{-14}\sigma^{3.3}$$

with a correlation coefficient of 1.00 for Al_2O_3/Al–7Si–0.6Mg composite, and

$$\dot{\varepsilon} = 10^{-14.5}\sigma^{3.6}$$

with a correlation coefficient of 0.98 for Al_2O_3/Al–5Si–3Cu–1Mg composite, where $\dot{\varepsilon}$ and σ are in s^{-1} and MPa, respectively. From the figure and the fitting equations, it is clear that the effect of stress on creep rate for the composites used in our study is not so strong as for aligned SiCw/6061 composite. For the two composites the values of n are 3.3 and 3.6, respectively, which are only a little larger than for solid-solution alloys. The reasons will be explained in the next paragraph.

3.3. Role of fibres during creep

It is well known that dislocation creep, grain boundary slip and diffusion creep are the three main possible creep mechanisms in metallic materials. Since the creep of ceramic fibre at 300 °C can be neglected, creep deformation of the MMC mainly consists of that of its matrix; in other words, the above three creep mechanisms are also the main creep mechanisms for the composites. However, the fibres in MMCs will strongly affect matrix creep deformation in the case of strong F–M interfaces.

Firstly, the fibres traversing grain boundaries efficiently resist grain boundary slips, so it is difficult to observe noticeable grain boundary slips in a region rich in fibres as shown in Fig. 6a. By contrast, in a region poor in fibres for the same specimen, grain boundary slips can be clearly seen as shown by Fig. 6b, in which the grain boundaries have been

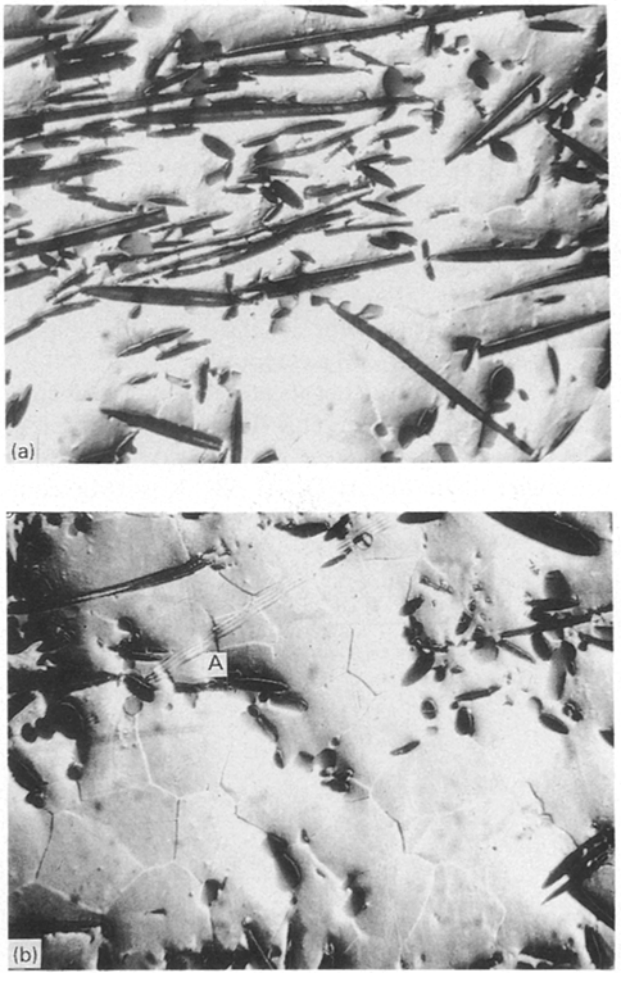

Figure 6 Grain boundaries displayed by creeping: (a) in a region rich in fibres and (b) in a region poor in fibres. × 1100.

revealed by creep rather than by etchant, and the lines labelled A were obviously displaced a little at a grain boundary. It follows that a small creep rate of the composites is related to this role of fibres.

Secondly, it has been well demonstrated that ceramic fibres in MMCs strongly resist dislocation glide, and a number of dislocations pile up in front of the fibres [14]. Evidently this role still exists even at elevated temperature, especially when the fibres are randomly distributed in the matrix. In this case, liberal glide of dislocations, in no matter which direction, is restricted to a very limited space, leading to so many dislocations piled up in front of the fibres that dislocation glide will be more and more difficult. This is a substantial creep strengthening mechanism, and its strengthening efficiency is much more significant than those in both particulate and unidirectional fibre MMCs. That is the main reason why a noticeable short-term negative creep occurred in the tests for the composites.

Of course, when the external load is high enough to overcome the resistance from stress fields induced by the piled-up dislocations in front of the fibres, the piled-up dislocations can move again by formation of dislocation loops around the fibres; at that moment the negative creep starts reducing. For the same reason, negative creep was reduced and even disappeared as the applied stresses were elevated enough as shown by Fig. 7. In this figure the first load increase was made when negative creep had occurred, but the negative creep still existed at increased loads (92 MPa); thus, after creeping at 92 MPa for 1.5 h, a second load increase from 92 to 106 MPa was made. Evidently the negative creep began to disappear at the second increased load and had completely disappeared at 118 MPa. It can be concluded that (i) the short-term negative creep did result from randomly oriented fibres resisting dislocation motions, and (ii) there is a critical stress for the presence of the negative creep, which is about 100 MPa for Al_2O_3/Al–7Si–0.6Mg composite (see Fig. 3c) and 110 MPa or so for Al_2O_3/Al–5Si–3Cu–1Mg composite.

The magnitudes of negative creep under different stress levels are given in Table III, from which it can be seen that the negative creep for Al_2O_3/Al–7Si–0.6Mg is smaller than for Al_2O_3/Al–5Si–3Cu–1Mg composite. This is because that there are more precipitates

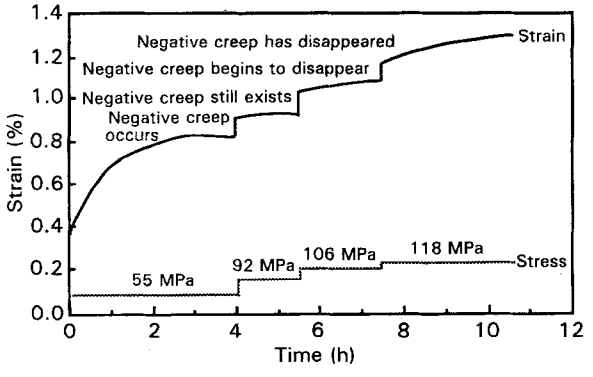

Figure 7 Creep curves at several stress levels and 300° for the same specimen of Al_2O_3/Al–5Si–3Cu–1Mg.

and intermetallic phases in the Al–5Si–3Cu–1Mg matrix, for example Si, Mg_2Si, $CuAl_2$, Al_2CuMg and other complex intermetallic compounds (Fig. 2a), but only Si and little Mg_2Si in Al–7Si–0.6Mg (Fig. 2b). Hence the resistance to dislocation motion in the Al_2O_3/Al–5Si–3Cu–1Mg composite was greater, so the negative creep and critical stress were therefore greater too.

The reason why n values of the composites are not so high as that of SiCw/6061 alloy composite is probably owing to the following two main differences between them: first of all, the dimensions of the alumina fibres (see Table I) are larger than those of SiC whisker (diameter 0.3–0.6 μm, length 5–15 μm) [15]; on the other hand, orientation of the alumina fibres in the matrices is random, while SiC whiskers in 6061 matrix are aligned, leaving a long passage for dislocation motion. The combination of these two facts leads to the large and sufficiently stable stress field induced by the piled-up dislocations in the two composites used in our study; a small increase of load or stress in a certain range cannot markedly affect dislocation creep. It can be imagined that if the applied stress was in the range above the critical stress, the n value would be increased.

Finally, fibres in MMCs are the main constituent carrying load and the load supported by the matrix is smaller than the applied normal stress; thus the creep takes place at smaller real stresses and the creep contributed by grain boundary slip is relatively increased, because the smaller the load, the more important the contribution to creep of grain slip.

All the above points are favourable for reducing the creep rate of the composites. Hence, generally speakking, the creep rate of fibre MMCs can be smaller by one order of magnitude relative to their matrix alloys alone.

3.4. Changes in microstructure

The microstructure of an elevated-temperature creep or stress-rupture test specimen rarely resembles the initial microstructure. Most materials are not thermodynamically stable; hence prolonged exposure under creep conditions can result in the precipitation of new phases, grain growth, and even physicochemical reaction between the fibres and the matrix in some MMC systems, when the temperature is elevated enough. Although many of the structural changes can be duplicated through simple heat treatment, some changes will only occur under the combined influence of stress and temperature. Microstructural changes due to the combined influence of temperature and stress are the most difficult to control. These changes enhance creep and therefore contribute to the observed strain.

Interfaces in the two composites are substantially composed of strong chemical bonds because of the presence of active excess Mg [16, 17]. However, a short contact time between the fibres and liquid matrix and a non-uniform temperature distribution in the casting during manufacturing the composites could lead to a heterogeneous F–M interface structure; some interfaces were in part mechanical bonds. At

Figure 8 F–M interface failed during creeping. × 1100.

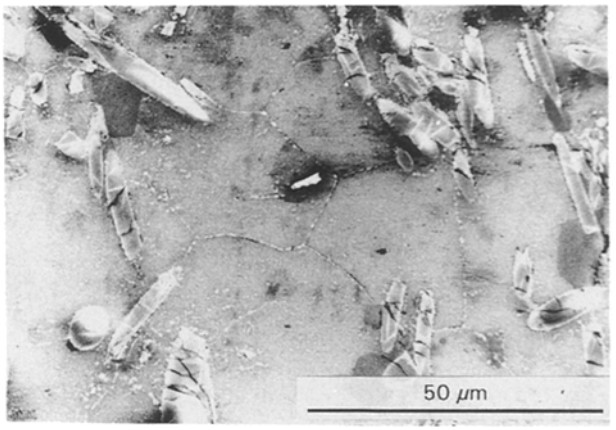

Figure 9 New phase precipitated during the creep (shown as small white points). × 1000.

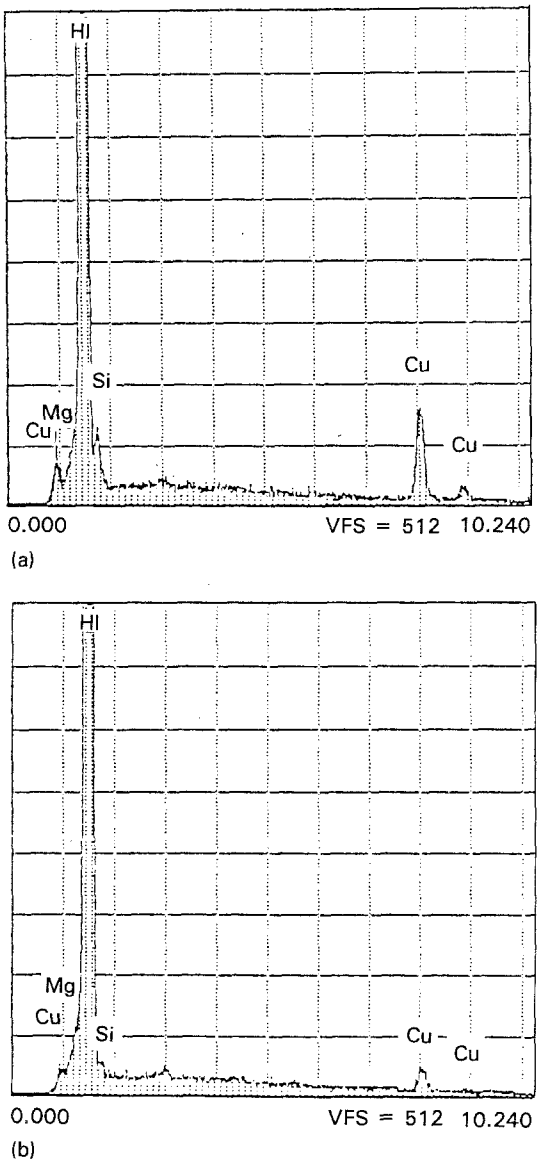

Figure 10 Chemical composition in the Al–5Si–3Cu–1Mg matrix (a) at a grain boundary and (b) in a region out of the grain boundary.

elevated temperature this kind of interface released the interlocking effects produced by differential contraction and roughened fibre surfaces; they then glided under stress action, and even failed as shown by Fig. 8.

As for the chemical stability of the composites used, the F–M interfaces were stable at 300 °C and no apparent chemical change at F–M interfaces was detected, because of a not too high temperature and the chemical inertness of Al_2O_3. However, after comparison with Fig. 2a, it is seen that some small new phases were precipitated from Al–5Si–3Cu–1Mg matrices during the creep tests as shown in Fig. 9. The chemical compositions of grain boundaries in the Al–5Si–3Cu–1Mg matrix was obviously changed: the precipitated small compounds contain more Cu and Si with respect to the matrix as indicated by microanalysis through the electron probe (Fig. 10). The chemical composition and the phase diagram being considered, the small precipitated phases are probably complex intermetallic compounds, such as $Cu_4Mg_5SiAl_x$; however, no evident change in the Al–7Si–0.6Mg matrix was detected. It can be concluded that the physicochemical stability of the Al–7Si–0.6Mg matrix is better than that of Al–5Si–3Cu–1Mg alloy matrix. It was because of this difference that the creep rate of Al–5Si–3Cu–1Mg alloy composite was a little larger than that of Al–7Si–0.6Mg alloy composite.

4. Conclusions

The presence of short-term negative creep in primary creep is an important feature for the composites, and results from randomly oriented fibres strongly resisting dislocation creep of the matrices. However, the extent of negative creep depends on both the applied stress and the nature of the material. There is a critical stress for the presence of short-term negative creep; when the applied stress had exceeded the critical value the negative creep disappeared. Fibres traversing grain boundaries can reinforce and resist grain-

boundary sliding at elevated temperature if the F–M interfaces are strong enough. The effect of stress on creep rate for the composites is not so strong as for unidirectional MMCs. During the creep, some intermetallic phases in the Al_2O_3/Al–5Si–3Cu–1Mg composite were precipitated and most of them segregated at grain boundaries, leading to a small increase in the creep rate.

References

1. S. NISHIDE, in "Mechanical Properties and Applications of MMC", Proceedings of Japanese–French workshop, Paris, February 1992, edited by S. Nishijima and C. Bathias (The Science and Technology Agency, Tokyo) p. 151.
2. S. T. MILEIKO, *J. Mater. Sci.* **5** (1970) 254.
3. D. McLEAN, *ibid.* **7** (1972) 98.
4. A. KELLY and K. N. STREET, *Proc. Roy. Soc.* **A328** (1972) 283.
5. H. LILHOLT, in "Relations Between Matrix and Composite Creep Behavior, Fatigue and Creep of Composite Materials", edited by H. Lilholt and R. Talreja (Risø National Laboratory, Roskilde, 1982) p. 63.
6. *Idem, Comp. Sci. Technol.* **22** (1985) 277.
7. M. McLEAN, in Proceedings of 5th International Conference on Composite Materials, edited by W. C. Harrigan, J. Strife and A. K. Dhingra (The Metallurgical Society, AIME, Warrendale, 1985) p. 37.
8. S. GOTO and M. McLEAN, *Acta Metall. Mater.* **39**(2) (1991) 153.
9. *Idem, ibid.* **39**(2) (1991) 153.
10. T. G. NIEH, *Metal Trans.* **15A** (1984) 139.
11. H. LILHOLT and M. TAYA, in Proceedings of International and European Conference on Composite Materials, Vol. 2, edited by F. L. Matthews, N. C. R. Buskell, J. M. Hodgkinson and J. Morton (Elsevier Applied Science, London, 1987) p. 2.234.
12. H. R. VOORHEES, in "Metals Handbook", 9th Edn, Vol. 8, edited by J. R. Newby *et al.* (American Society for Metals, 1985) p. 329.
13. A. L. KEARNEY, in "Metals Handbook", 10th Edn, Vol. 2 (ASM International, 1990) p. 153.
14. V. D. SCOTT, R. L. TRUMPER and M. YAUNG, *Compo. Sci. Technol.* **42** (1991) 251.
15. I. IMAZN and T. TAKENAKA, in "Mechanical Properties and Applications of MMC", Proceedings of Japanese–French workshop, Paris, February 1992, edited by S. Nishijima and C. Bathias, p. 19.
16. A. D. McLEOD, in Proceedings of Conference on Fabrication of Particulate-Reinforced Metal Composites, Montreal September 1990 (ASM International) p. 25.
17. P. K. GHOSH and S. RAY, *ibid.* p. 30.

Received 17 December 1992
and accepted 9 February 1994